Arab J Sci Eng (2017) 42:3055–3063
DOI 10.1007/s13369-017-2525-z

RESEARCH ARTICLE - SYSTEMS ENGINEERING

Robust Fault-Tolerant Control of Wind Turbine Systems Against Actuator and Sensor Faults

Montadher S. Shaker[1] · **Asaad A. Kraidi**[1]

Received: 2 September 2016 / Accepted: 10 April 2017 / Published online: 19 April 2017

Abstract This paper develops a novel observer-based fault-tolerant control (FTC) for wind turbine blade pitch system subjected to simultaneous actuator and sensor faults. The main contribution of this paper is the proposal of new architecture based on a combination of sliding mode control (SMC) and a proportional–proportional–integral-observer (PPIO) to provide tight reference blade pitch angle tracking regardless of the effects of actuator and sensor faults. Within this architecture, an integral sliding surface-based SMC (ISMC) has been developed to stabilize tracking error dynamics during sliding phase while the system is subjected to actuator faults. The robust PPIO-based sensor fault estimation is utilized to compensate sensor fault from the input of ISMC and thereby guarantee closed-loop system robustness against actuator and sensor faults. Stability analysis has clearly demonstrated using linear matrix inequality and Lyapunov approach. The proposed method is applied to 4.8 MW wind turbine FTC benchmark model.

Keywords Sliding mode control · Proportional–proportional–integral-observer (PPIO) · Wind turbine control · Robust control · Robust fault estimation

1 Introduction

The last decades have witnessed an increasing interest in maximizing the percentage of green energy over the fossil fuel energy resources. However, installation and maintenance costs are real challenges to the rapid growth in the use of green energy [1]. Recently, research studies paid great attention into methods that relax these challenges. In this context, wind turbine control systems have played vital role in maximizing the conversion efficiency of wind energy into electrical energy [2,3]. Specifically, research into FTC methods offer significant reduction of plant downtime and, thus, avoid the unscheduled maintenance costs [4–9].

In this perspective, [10] presents the recent developments that aim to increase reliability and availability of large scale wind turbine systems. The authors of [11] assisted the wind turbine baseline controller by a linear parameter varying (LPV) descriptor observer to provide closed-loop system robustness against sensor fault. In [12], an FTC scheme exploits disturbance compensator approach to robust control design has been developed to tolerate the effect of high air content, pump wear, and hydraulic leakage faults of pitch actuator system. The design of fault tolerant LPV controller has been addressed in [13] where the performance of active and passive fault-tolerant controllers designed to tolerate pitch system fault and model parameter uncertainty has been compared. The authors in [14] adopt the Takagi-Sugeno fuzzy approach to synthesis a multiple-model active sensor FTC strategy for 4.8 MW wind turbine system. The proposal generates observer-based sensor fault estimate signals to compensate the effects of generator speed and/or rotor speed sensor faults from the controller inputs. The simulation results confirm the ability of the proposed FTC strategy to maintain the nominal control system response over a wide variety of sensor fault scenarios. In [15], an interesting fault-tolerant dynamic output feedback fuzzy controller has been developed for wind turbine systems operating in the low range of wind speed. The proposed controller guarantees maximum conversion efficiency regardless of the effects of

✉ Montadher S. Shaker
30211@uotechnology.edu.iq; montadher_979@yahoo.com

Asaad A. Kraidi
asaadabdlbari@gmail.com

[1] Department of Electrical Engineering, University of Technology, Baghdad, Iraq

sensor faults. Badihi et al. [4] integrates model-based fault detection and diagnosis scheme with proportional integral fuzzy controller to ensure closed-loop system robustness against sensor faults.

On the other hand, several publications have shown interest in the use of the relative design simplicity and the robustness of SMC for wind turbine control applications. The work in [8] exploits the robustness of SMC against matched uncertainty to tolerate the effect of generator torque scale fault and thereby preserve the conversion efficiency at its optimal value. A chattering free second-order SMC-based wind turbines fault ride-through capability enhancement has been developed by [16] as an improved solution to avoid the negative effects of SMC chattering.

While the FTC proposed in [12] tackles the high air content, pump wear, and hydraulic leakage faults which have direct effects on the transient response performance of the pitch actuator system, the control system lacks the robustness against sensor fault. Similarly, the passive and active FTC proposed in [13] has been designed under the assumption that the sensors are fault free. The work in [11,15,17,18] focuses only on compensating sensor faults from the input of the baseline controllers.

Compared with the aforementioned literature of FTC-based sustainable wind turbine control, the main contribution of this paper is the proposal of a new FTC loop capable of maintaining nominal pitch actuator response even when the system is affected by simultaneous actuator and sensor faults. Within this framework, the inherent robustness of SMC is exploited to ensure acceptable tracking performance when the pitch actuator is affected by high air content or hydraulic leakage faults. On the other hand, the PPIO is employed in this proposal to provide sensor fault estimation signal to actively compensate sensor faults.

2 Wind Turbine Model and Fault Analysis

Generally, wind turbine models are obtained via combining its individual component models. Specifically, in this paper, the drive train subsystem includes a flexible rotor side shaft, generator side shaft, and a gearbox. Its model is given as:

$$\begin{bmatrix} \dot{\omega}_r \\ \dot{\omega}_g \\ \dot{\theta} \end{bmatrix} = \begin{bmatrix} a_{11} & a_{12} & a_{13} \\ a_{21} & a_{22} & a_{23} \\ a_{31} & a_{32} & a_{33} \end{bmatrix} \begin{bmatrix} \omega_r \\ \omega_g \\ \theta \end{bmatrix} + \begin{bmatrix} b_{11} & 0 \\ 0 & b_{22} \\ 0 & 0 \end{bmatrix} \begin{bmatrix} T_a \\ T_g \end{bmatrix}$$

$$a_{11} = -\frac{(B_{dt} + B_r)}{J_r}, \quad a_{12} = \frac{B_{dt}}{n_g J_r}, \quad a_{13} = -\frac{K_{dt}}{J_r},$$

$$a_{21} = \frac{B_{dt}}{n_g J_g}, \quad a_{22} = -\frac{\left(B_{dt} + n_g B_g\right)}{n_g^2 J_g}, \quad a_{21} = \frac{K_{dt}}{n_g J_g},$$

$$a_{31} = 1, \quad a_{32} = -\frac{1}{n_g}, \quad a_{33} = 0, \quad b_{11} = \frac{1}{J_r},$$

$$b_{22} = -\frac{1}{J_g} \tag{1}$$

where J_r, B_r, J_g, ω_g, T_g, B_g, n_g, K_{dt}, B_{dt}, θ and T_a are the rotor inertia, the rotor external damping, the generator inertia, the generator speed, the generator torque, generator, external damping, the gearbox ratio, the torsion stiffness, the torsion damping coefficient, the torsion angle, and T_a is the aerodynamic torque and has the form:

$$T_a = 0.5\rho_a \pi R^2 C_p(\lambda, \beta) \frac{v^3}{\omega_r} \tag{2}$$

where ω_r, β, and v are the rotor speed, the blade pitch angle, and the wind speed respectively. ρ_a, R, and C_p are the air density, the radius of the rotor and the power coefficient. The C_p depends on the blade pitch angle and the tip-speed-ratio (λ) defined as:

$$\lambda = \omega_r R / v \tag{3}$$

The electrical subsystem is given by the following linear relation

$$\dot{T}_g = -\frac{1}{\tau_g} T_g + \frac{1}{\tau_g} T_{gr} \tag{4}$$

where T_{gr} is the reference generator torque signal and τ_g is the time constant.

The hydraulic pitch system for each blade pitch system is modeled as a closed-loop 2nd order transfer function between the measured pitch angle β and its reference β_r. The state space model of the system can be written as:

$$\left.\begin{aligned} \dot{x} &= Ax + B\beta_r + D\psi(x, \beta_r) \\ y &= Cx \end{aligned}\right\} \tag{5}$$

where

$$A = \begin{bmatrix} 0 & 1 \\ -\omega_n^2 & -2\zeta\omega_n \end{bmatrix}, \quad B = \begin{bmatrix} 0 \\ \omega_n^2 \end{bmatrix},$$

$$C = \begin{bmatrix} 1 & 0 \end{bmatrix}, \quad D = \begin{bmatrix} 0 \\ 1 \end{bmatrix}$$

$x = \begin{bmatrix} \beta & \dot{\beta} \end{bmatrix}^T$ is the state vector, $\psi(x, \beta_r)$ represents system and/or actuator fault, ζ is the damping factor, and ω_n is the natural frequency. The nominal values of the parameters are $\zeta = 0.6$ and $\omega_n = 11.11$ rad/s [7].

From system reliability standing point, faults could affect any part of the wind turbine system. Therefore, robust control objective is to tolerate the effects of wind turbine faults so that desired closed-loop performance can be maintained. Analyses of some fault scenarios are given below:

- *Rotor speed sensor scaling fault:* this fault drives the turbine away from the optimal operation. The control signal, generated based on faulty measurement, will steer the turbine away from its optimal rotational speed (ω_{ropt}). On the other hand, at the high range of wind speed, the controller steer the turbine below or above the rated rotational speed.
- *Stuck rotor speed sensor fault:* based on the difference between of the stuck fault magnitude and ω_{ropt}, the controller will either force the system toward the cut-off region whenever ω_{ropt} is lower than the rotor stuck measurement or simply release the turbine to rotate without control if ω_{ropt} is higher than the stuck fault.
- *Generator torque scaling fault:* in this fault scenario the controller minimizes the difference between the T_{gr} and the measured generator torque T_{gm}. In fact, T_{gm} is obtained via soft sensing. Therefore, measurement fault will decrease the power conversion efficiency.
- *Blade pitch sensor scaling fault:* clearly, the blade pitch controller minimizes the difference between the β_{r} and β. Thus, faulty β causes incorrect control of the rotor blades and thereby unevenness in the forces of the rotor. Clearly, this will increase the probability of turbine structure damage.
- *Stuck blade pitch sensor fault:* depending on the magnitude of stuck fault, the controller will pitch the blade toward the maximum or minimum magnitude of the blade pitch angle. Again, this could cause system damage due to the increased structural loads on the wind turbine.
- *Blade pitch actuator fault:* This fault scenario is attributed to the drop of oil pressure or the increase in air content of the pitch actuator. This fault will directly affect the tracking performance of the actuator.

Remark 1 In the blade pitch system, the drop of oil pressure fault or the increase in air content fault is represented as a deviation in the nominal values of the parameters ζ and ω_{n} [7,19]. Thus, the model parameters (ζ and ω_{n}) of (5) could have the following generalized form:

$$\omega_{\text{n}}^2 = \omega_{\text{no}}^2 + \Delta\left(\omega_{\text{nf}}^2 - \omega_{\text{no}}^2\right)$$
$$2\zeta\omega_{\text{n}} = 2\zeta_{\text{o}}\omega_{\text{no}} + \Delta\left(2\zeta_{\text{f}}\omega_{\text{nf}} - 2\zeta\omega_{\text{no}}\right)$$

where $\Delta \in \left[0\ 1\right]$ is the fault severity parameter. Specifically, $\Delta = 0$ corresponds to fault-free system and $\Delta = 1$ corresponds to complete faulty system. The parameters $\zeta_{\text{o}}, \omega_{\text{no}}$, ζ, ω_{n} and $\zeta_{\text{f}}, \omega_{\text{nf}}$ are the nominal, generalized and faulty model coefficients respectively. Hence, the coefficients of (5) become:

$$A \in R^{(n*n)} = \begin{bmatrix} 0 & 1 \\ -\omega_{\text{no}}^2 & -2\zeta\omega_{\text{no}} \end{bmatrix},\ B \in R^{(n*m_b)} = \begin{bmatrix} 0 \\ \omega_{\text{no}}^2 \end{bmatrix},$$

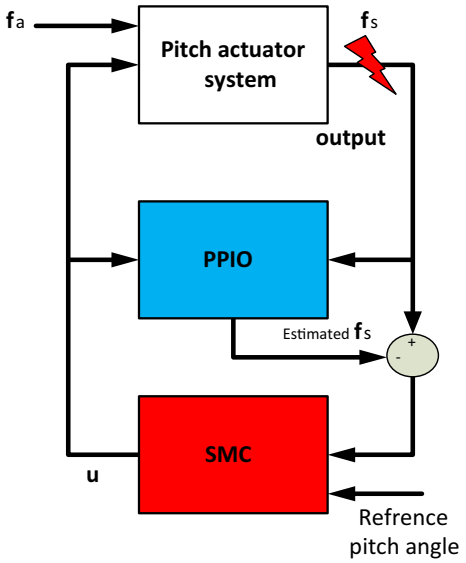

Fig. 1 The proposed control structure

$$C \in R^{(r*n)} = \begin{bmatrix} 1\ 0 \end{bmatrix},\ D \in R^{(n*d)} = \begin{bmatrix} 0 \\ 1 \end{bmatrix}$$
$$\psi(x, \beta_{\text{r}}) = \Delta(2\zeta_{\text{o}}\omega_{\text{no}} - 2\zeta_{\text{f}}\omega_{\text{nf}})\dot{\beta} + \Delta(\omega_{\text{no}}^2 - \omega_{\text{nf}}^2)\beta \ldots$$
$$-\Delta(\omega_{\text{no}}^2 - \omega_{\text{nf}}^2)\beta_{\text{r}}$$

Assumption 1 the function $\psi(x, \beta_{\text{r}})$ satisfies the condition $\|\psi(x, \beta_{\text{r}})\| \leq \varphi$. Where the scalar φ represents the known upper bound of $\psi(x, \beta_{\text{r}})$. Practically, this is an acceptable assumption since all the variables of $\psi(x, \beta_{\text{r}})$ are bounded.

In this work, the pitch actuator system is studied since its faults have the highest failure rate [7].

3 The Proposed Control Structure

This section presents the proposed control structure that exploits the robustness of SMC assisted by PPIO within a feedback loop. Specifically, the next subsection presents the SMC design methodology for the pitch actuator system affected by actuator and sensor faults. On the other hand, Sect. 3.2 will present a new control structure that combines the SMC and PPIO in order to tolerate simultaneous actuator and sensor faults (see Fig. 1).

3.1 Sliding Mode Controller Design

The ability of SMC to compensate matched disturbances has been clearly investigated in the robust control literature. Briefly, the SMC design procedure encompasses two steps [20,21]; (1) the sliding surface design to which the states

are confined during the sliding phase. (2) The control signal that makes the sliding surface attracts the states during the reaching phase. In the SMC framework, the control law has two feedback control terms; (i) a linear control term, and (ii) a discontinuous term. While the linear control term guarantees the reachability condition, the discontinuous control term ensures the sliding condition.

The rest of this section presents the ISMC design steps for pitch actuator subsystem (5).

Remark 2 1. The system given in (5) represents the closed-loop model of the blade pitch actuator system. According to [7,19], a faulty pitch system, e.g., the drop of oil pressure, can be modeled as a change in the parameters ζ and ω_n of this system.
2. In this section, the sliding mode controller can be considered as a supplementary controller designed for tolerating the effects of pitch actuator faults and thereby maintaining the fault-free system response unchanged.

The dynamics of the error $e = \beta - \beta_r$ of the pitch actuator system combined with the supplementary controller is given as:

$$\left.\begin{aligned} \dot{e} &= \dot{\beta} - \dot{\beta}_r \\ \ddot{e} &= -2\zeta\omega_{no}\dot{\beta} - \omega_{no}^2\beta - \ddot{\beta}_r + \omega_{no}^2\beta_r \ldots \\ &\quad + \omega_{no}^2 u_{ftc}^{smc} + \psi(x, \beta_r) \end{aligned}\right\} \tag{6}$$

The first design step is to propose a sliding surface capable of achieving control goals whenever the system reaches this surface. The following integral surface has been proposed for the blade pitch system in (5):

$$S = \dot{e} + k_1 e + k_2 \int e \tag{7}$$

The proposed sliding surface has the form of Eq. (7) to bring the effect of the controlled input to the $\dot{S}$ term and thereby achieving the reachability and sliding conditions. Moreover, it is clear that while the system is in the sliding mode (i.e. $S = \dot{S} = 0$), the unique solution occurs for ($e = 0$). Furthermore, while the system trajectory is in the sliding manifold, the dynamics are governed by the design parameters (k_1, k_2) which can be selected such that the desired tracking performance is achieved.

Now, the challenge is to find the control action that achieves the objectives of satisfying the reachability condition and the sliding condition.

To guarantee the reachability condition, the control signal must achieve the following condition:

$$S\dot{S} \le -\varepsilon |S| \tag{8}$$

where ε is small positive constant. Using (7) gives the following expression of $\dot{S}$:

$$\begin{aligned} \dot{S} &= \ddot{e} + k_1\dot{e} + k_2 e \\ &= -2\zeta\omega_{no}\dot{\beta} - \omega_{no}^2\beta - \ddot{\beta}_r + \omega_{no}^2 u_{ftc}^{smc} + \omega_{no}^2\beta_r \ldots \\ &\quad + \psi(x, \beta_r) + k_1\dot{e} + k_2 e \end{aligned} \tag{9}$$

Hence, when the system reaches the sliding manifold (i.e., $S = \dot{S} = 0$), the equivalent control signal could have the form:

$$\begin{aligned} u_{eq} = \frac{1}{\omega_{no}^2}\Big[&2\zeta\omega_{no}\dot{\beta} + \omega_{no}^2\beta + \ddot{\beta}_r - \omega_{no}^2\beta_r \ldots \\ &-\psi(x, \beta_r) - k_1\dot{e} - k_2 e \end{aligned} \tag{10}$$

A more realistic expression for the equivalent control (10) could be of the form:

$$\begin{aligned} u_{ftc}^{smc} = \frac{1}{\omega_{no}^2}\Big[&2\zeta\omega_{no}\dot{\beta} + \omega_{no}^2\beta + \ddot{\beta}_r - \omega_{no}^2\beta_r + \cdots \\ &k_1(\dot{\beta}_r - \dot{\beta}) + k_2(\beta_r - \beta) - \eta\,\mathrm{sgn}(S)\Big] \end{aligned} \tag{11}$$

where $\eta = \varphi + \varepsilon$. Substituting (11) into (9) gives:

$$\dot{S} = \psi(x, \beta_r) - (\varphi + \varepsilon)\,\mathrm{sgn}(S) \tag{12}$$

Multiplying both sides of equality (12) by the sliding variable (S) gives the reachability condition (8).

$$S\dot{S} \le -\varepsilon S\,\mathrm{sgn}(S) \Rightarrow S\dot{S} \le -\varepsilon |S| \tag{13}$$

Hence, regardless the effects of low pressure fault and/or increase air content fault, the supplementary sliding mode controller ensures accurate tracking of the reference pitch angle.

It should be noted that the ISMC design procedure is addressed in terms of finding a control law for the input u_{ftc}^{smc} that verifies the reachability and sliding conditions. Subsequently, with reference to inequality (13), since $S\dot{S} = \frac{1}{2}\frac{d}{dt}S^2$, it follows that the function $V(S) = \frac{1}{2}S^2$ is a Lyapunov function for the sliding dynamic S

Remark 3
- Although the proposed controller (11) is capable of maintaining robust closed-loop tracking performance against some fault scenarios, the sensor fault has direct effects on the sliding surface (7) and hence cannot be tolerated using (11).
- To avoid the chattering accompanied with sliding motion, a well-known approximation to the function $sgn(S)$ is given by $sgn(S) = \frac{S}{|S|+\tau}$ where τ is a small positive constant. This will ensure the sliding motion to be in the vicinity of the line($S = 0$) [22].
- The SMC based on surface (7) guarantees closed-loop robustness against the matched and mismatched uncertainty components of the pitch actuator system. For

instance, suppose the system (6) is affected by mismatched uncertainty (i.e., $\dot{e} = \dot{\beta} - \dot{\beta}_r + d$ where d represents mismatched uncertainty that satisfies $\lim_{t\to\infty} \dot{d} = 0$). It should be noted that while sliding, the dynamics of system (6) become $(\ddot{e} + k_1\dot{e} + k_2 e = \dot{d})$ which is homogeneous differential equation since $\lim_{t\to\infty} \dot{d} = 0$. This implies that the state in (6) moves toward the equilibrium point asymptotically regardless the effect of unmatched uncertainty.

3.2 PPIO-Based Sensor Fault Estimation

In this section, the fault estimation/compensation approach to FTC is nominated to correct the faulty blade pitch angle sensor. A proportional state observer augmented by proportion–integral feedback term for fault estimation is proposed to provide accurate estimates for wider ranges of sensor fault scenarios. The model of the actuator system with sensor fault can be of the following form:

$$\left.\begin{aligned} \dot{x} &= Ax + Bu_{\text{ftc}}^{\text{smc}} + D\psi(x, \beta_r) \\ y &= Cx + D_s f_s \end{aligned}\right\} \tag{14}$$

where $D_s = \begin{bmatrix} 1 & 0 \end{bmatrix}^T$ and f_s is the unknown sensor fault signal. To cope with the sensor fault estimation problem, an augmented system assembles the model (14) and an output filter is constructed. The output filter is represented by the following form:

$$\dot{x}_s = -A_s x_s + A_s C x + A_s D_s f_s \tag{15}$$

where $-A_s \in R^{l*l}$ is a stable filter matrix. The augmented model is given as follows:

$$\left.\begin{aligned} \dot{\bar{x}} &= \bar{A}\bar{x} + \bar{B}u_{\text{ftc}}^{\text{smc}} + \bar{D}\psi(x, \beta_r) + \bar{D}_s f_s \\ \bar{y} &= \bar{C}\bar{x} \end{aligned}\right\} \tag{16}$$

$$\bar{A} = \begin{bmatrix} A & 0 \\ A_s C & -A_s \end{bmatrix}, \bar{x} = \begin{bmatrix} x \\ x_s \end{bmatrix}, \bar{B} = \begin{bmatrix} B \\ 0 \end{bmatrix}, \bar{D} = \begin{bmatrix} D \\ 0 \end{bmatrix},$$
$$\bar{D}_s = \begin{bmatrix} 0 \\ A_s D_s \end{bmatrix}, \bar{C} = \begin{bmatrix} 0 & I_l \end{bmatrix}$$

As illustrated in Remark 3, in order to guarantee robustness against sensor fault, the proposed control strategy requires compensation of the sensor faults affecting the system. The PPIO for the system (16) is given as:

$$\left.\begin{aligned} \dot{\hat{x}} &= \bar{A}\hat{x} + \bar{B}u_{\text{ftc}}^{\text{smc}} + \bar{D}_s\hat{f}_s + L\bar{C}e_x \\ \hat{y} &= \bar{C}\hat{x} \\ \dot{\hat{f}}_s &= \rho\left[K_1\bar{C}\dot{e}_x + K_2\bar{C}e_x\right] \end{aligned}\right\} \tag{17}$$

where $\hat{x}$ is the estimated state, $\hat{y}$ is the estimated output, $e_y = \bar{y} - \hat{y} = \bar{C}e_x$, $K_1 \in R^{(m_f*r)}$, $K_2 \in R^{(m_f*r)}$ are the proportional and integral gains, respectively, and $\rho \in R^{(m_f*m_f)}$ is a symmetric positive definite matrix. Subtracting the observer in (17) from the system (16), the state estimation error will be defined as:

$$\left.\begin{aligned} \dot{e}_x &= \left(\bar{A} - L\bar{C}\right)e_x + \bar{D}\psi(x, \beta_r) + \bar{D}_s e_{fs} \\ e_y &= \bar{C}e_x \end{aligned}\right\} \tag{18}$$

where $e_{fs} = f_s - \hat{f}_s$. Using (18), the fault estimation error dynamics will become:

$$\left.\begin{aligned} \dot{e}_{fs} &= \dot{f}_s - \dot{\hat{f}}_s \\ \dot{e}_{fs} &= \dot{f}_s - \rho K_1\bar{C}\bar{A}e_x + \rho K_1\bar{C}L\bar{C}e_x - \rho K_2\bar{C}e_x \ldots \\ &\qquad -\rho K_1\bar{C}\bar{D}_s e_{fs} - \rho K_1\bar{C}\bar{D}\psi \end{aligned}\right\} \tag{19}$$

by combining (18) and (19), the state and fault error dynamics can be assembled as in (20):

$$\dot{\tilde{e}}_a(t) = \tilde{A}\tilde{e}_a + \tilde{N}\tilde{z} \tag{20}$$

where

$$\tilde{A} = \begin{bmatrix} \bar{A} - L\bar{C} & \bar{D}_s \\ -\rho K_1\bar{C}\bar{A} + PK_1\bar{C}L\bar{C} - \rho K_2\bar{C} & -\rho K_1\bar{C}\bar{D}_s \end{bmatrix},$$
$$\tilde{z} = \begin{bmatrix} \psi \\ \dot{f}_s \end{bmatrix}, \quad \tilde{N} = \begin{bmatrix} \bar{D} & 0 \\ -\rho K_1\bar{C}\bar{D} & I \end{bmatrix} \tilde{e}_a = \begin{bmatrix} e_x \\ e_{fs} \end{bmatrix}$$

Now, the objective is to compute the gains L, K_1 and K_2 that attenuate the effects of the input $\tilde{z}$ on the estimation error via minimizing the $\mathcal{L}_2$ norm $\|\tilde{z}\|_2$, which should stay below a desired level γ.

Theorem *The augmented estimation error in (20) is stable and the $\mathcal{L}_2$ performance is guaranteed with an attenuation level γ, provided that the signals $\left(\dot{f}_s, \psi\right)$, are bounded, rank $(\bar{C}\bar{D}_s) = m_f$, and the pair $(\bar{A}, \bar{C})$ is observable, if there exists a symmetric positive definite matrices P_1, ρ^{-1} and G, matrices H, K_1 and K_2, and a scalar μ satisfying the following LMI constraint*

Minimize $\bar{\gamma}$ such that

$$\begin{bmatrix} \varphi_{11} & \varphi_{12} & \varphi_{13} & \varphi_{14} & 0 & \varphi_{16} & 0 \\ * & \varphi_{22} & \varphi_{23} & \varphi_{24} & \varphi_{25} & 0 & 0 \\ * & * & -\bar{\gamma}I & 0 & 0 & 0 & 0 \\ * & * & * & -\bar{\gamma}I & 0 & 0 & 0 \\ * & * & * & * & -G^{-1} & 0 & 0 \\ * & * & * & * & * & -2\mu P_1 & \mu I \\ * & * & * & * & * & * & -G \end{bmatrix} < 0 \tag{21}$$

where w_1 and w_2 are weighting matrices, and

$$L = P_1^{-1}H, \gamma = \sqrt{\bar{\gamma}}$$
$$\varphi_{11} = P_1\bar{A} + \left(P_1\bar{A}\right)^T - H\bar{C} - \left(H\bar{C}\right)^T + w_1$$
$$\varphi_{12} = P_1\bar{D}_s + \bar{A}^T\bar{C}^T K_1^T - \bar{C}^T K_2^T, \varphi_{13} = P_1\bar{D}_s,$$
$$\varphi_{16} = (H\bar{C})^T, \varphi_{22} = -K_1\bar{C}\bar{D}_s - \left(K_1\bar{C}\bar{D}_s\right)^T + w_2$$
$$\varphi_{23} = -K_1\bar{C}\bar{D}, \varphi_{24} = \rho^{-1}, \varphi_{25} = K_1\bar{C}$$

Proof see [23]

Remark 4
- Based on the available information of $\bar{D}_s$ and $\bar{D}$, the inequality (21) attenuates the effects of the disturbance ($\tilde{z}$) on fault estimation signal via L_2 norm minimization.
- The robustness of the sliding motion against faulty measurements is assured via integrating the ISMC by PPIO responsible for estimating sensor faults as shown in Fig. 1.
- By constructing the augmented system in Eq. 16, this paper has extended the linear matrix inequality (LMI) design algorithm of PPIO-based actuator fault estimation, proposed recently in [23], to the case of sensor fault estimation.

4 Simulation Results

The aim of this section is to verify the effectiveness of the proposed control scheme (Fig. 1) for the blade pitch actuator of the wind turbine FTC benchmark model [7,19].

Remark 5
- Form design complexity standing point, the proposed ISMC makes use of the available output data and hence the complexity of observer-based state feedback based SMC is avoided.
- A filtered derivative of the form $(\frac{s}{T_f s+1})$ could be used to approximate the derivative in (7) where T_f is a positive scalar that can be selected to attain acceptable approximation.
- Practical implementation of sliding mode controller has been addressed in several research papers for mechanical and electrical systems using field programmable gate arrays [24] or digital signal processing system [25].

The first design step of the controller (11) is to determine the switching gain (η) and the sliding surface parameters (k_1, k_2). Satisfying assumption 1 ensures a sliding motion governed by the following second-order dynamics:

$$0 = \ddot{e} + k_1\dot{e} + k_2 e \tag{22}$$

Specifically, the design parameter $\eta = 50$ is selected to satisfy the reachability condition.

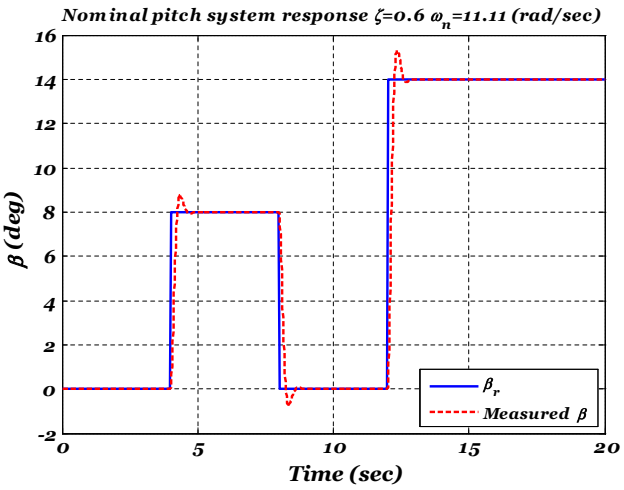

Fig. 2 The tracking performance of the pitch actuator system

Additionally, the performance parameters of the error system, governed by k_1 and k_2, are adopted to preserve the nominal time response of the pitch actuator (i.e., $\zeta_o = 0.6$ and $\omega_{no} = 11.11$ rad/s). Specifically, the sliding surface parameters (k_1, k_2) can be selected such that the error dynamics satisfy specific bound on transient response characteristics such as the settling time (T_s) and the peak time (T_p) [26]:

$$T_s = \frac{4}{\zeta_o\omega_{no}} = \frac{8}{k_1}, (T_p)^2 = \frac{\pi^2}{\omega_{no}^2(1-\zeta_o^2)} = \frac{\pi^2}{k_2(1-\zeta_o^2)}.$$

Figure 2 shows the nominal tracking response of the 2nd order blade actuator system to a multilevel reference pitch angle.

It is expected that the model parameter faults, i.e., the effect of low oil pressure and/or increase air content fault, will disturb the transient performance of the pitch actuator system. Consequently, these faults will limit the blade actuator tracking capability of the reference pitch angle. Figures 3 and 4 demonstrate the blade actuator tracking performance for two sets of faulty model parameters $\zeta = 0.25$, $\omega_n = 5.73$ rad/s and $\zeta = 0.9$, $\omega_n = 3.42$ rad/s respectively.

The purpose of the fault-tolerant controller is to force the faulty system to follow as closely as possible the response of the nominal (i.e., fault-free) system. Specifically, while the effects of model parameter fault, the proposed ISMC should maintain the nominal time response characteristics (i.e., settling time, peak time, rise time, and maximum overshoot). The effectiveness of the proposed ISMC is shown in Figs. 5 and 6.

On the other hand, the ISMC shows inability to tolerate the effects of sensor faults. This is because the generated control signal is based on faulty measurement and hence the controller minimizes the error $e = (\beta + f_s) - \beta_r$. Hence, when the ISMC makes $e = 0 = (\beta + f_s) - \beta_r$, the actual pitch

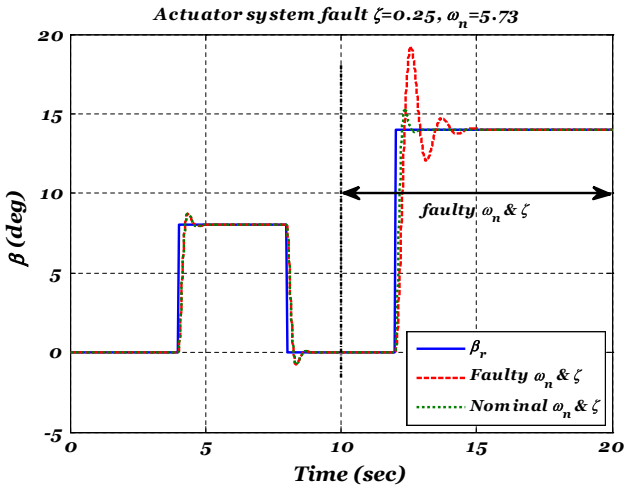

Fig. 3 The tracking performance of the faulty blade actuator system ($\zeta = 0.25 \quad \omega_{\mathrm{n}} = 5.73\,\mathrm{rad/s}$)

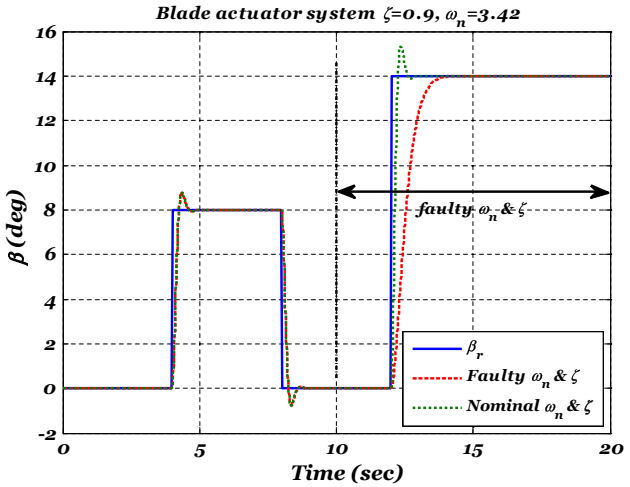

Fig. 4 The tracking performance of the faulty blade actuator system ($\zeta = 0.9 \quad \omega_{\mathrm{n}} = 3.42\,\mathrm{rad/s}$)

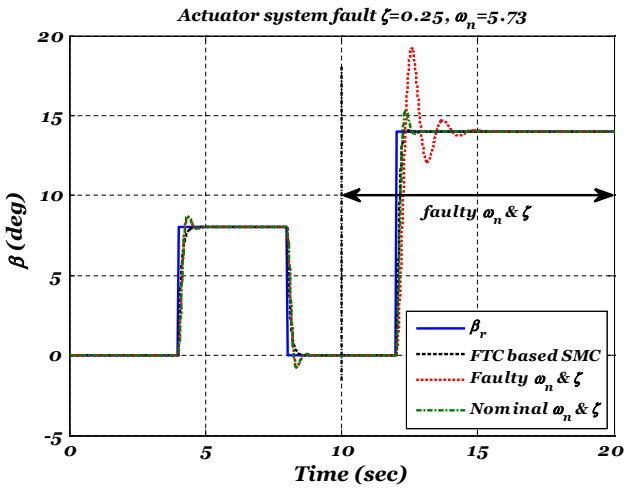

Fig. 5 The SMC performance of the faulty pitch actuator system ($\zeta = 0.25\ \omega_{\mathrm{n}} = 5.73\,\mathrm{rad/s}$)

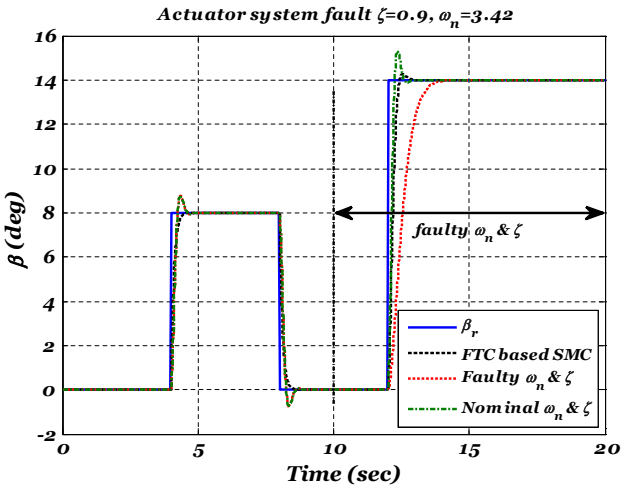

Fig. 6 The SMC performance of the faulty pitch actuator system ($\zeta = 0.9\,\omega_{\mathrm{n}} = 3.42\,\mathrm{rad/s}$)

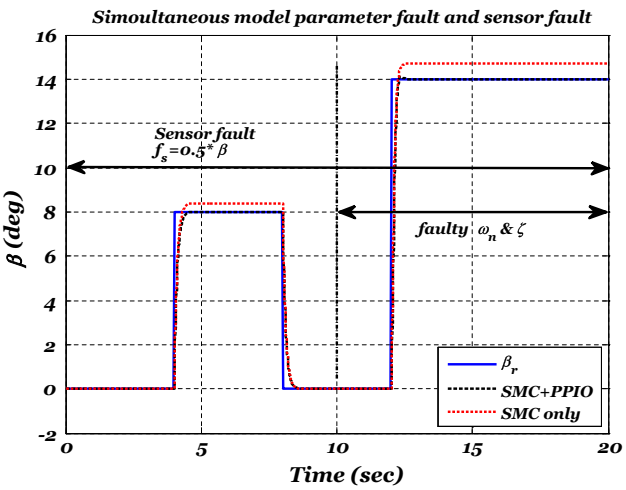

Fig. 7 The integrated SMC+PPIO performance against simultaneous actuator system fault ($\zeta = 0.25\,\omega_{\mathrm{n}} = 5.73\,\mathrm{rad/s}$) and sensor fault ($f_{\mathrm{s}} = 0.5\beta$)

angle is $\beta = \beta_{\mathrm{r}} - f_{\mathrm{s}}$. Therefore, it is suggested to integrate the ISMC with PPIO in order to provide fault tolerance against simultaneous parameter and sensor faults. Solving the LMI constraints of the PPIO gives the following values:

$$G = \begin{bmatrix} 8 & 0 & 0 \\ 0 & 8 & 0 \\ 0 & 0 & 8 \end{bmatrix}, \ \rho = 0.1, \ A_{\mathrm{s}} = 10, \ \gamma = 0.3549,$$

$$L = \begin{bmatrix} 0.4122 & 0.2456 & -0.6107 \end{bmatrix}^T,$$

$$K_1 = 1.1052, \quad \text{and} \quad K_2 = 82.2216$$

Figure 7 clarifies the effect of the sensor fault and the performance of the proposed integrated ISMC and PPIO.

It should be noted that the sensor fault ($D_{\mathrm{s}} f_{\mathrm{s}} = 0.5\beta$) has been tolerated using estimation and compensation approach

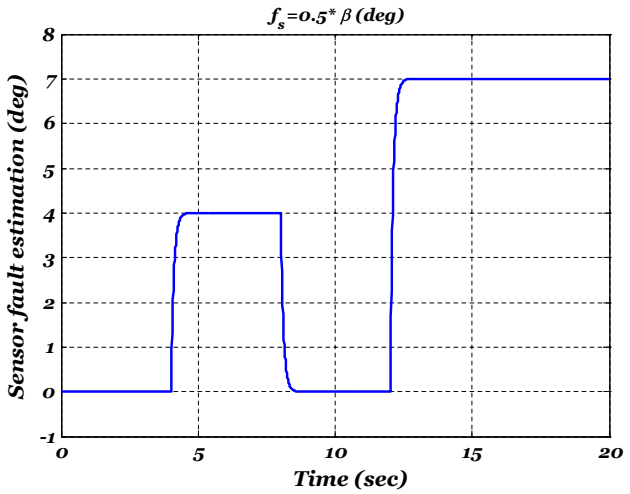

Fig. 8 Sensor fault estimation using PPIO

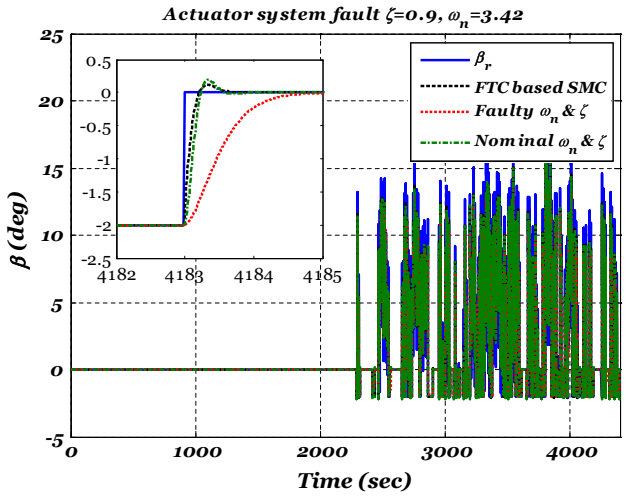

Fig. 9 The tracking performance of the faulty pitch actuator system ($\zeta = 0.9\,\omega_n = 3.42\,\text{rad/s}$) under realistic wind data

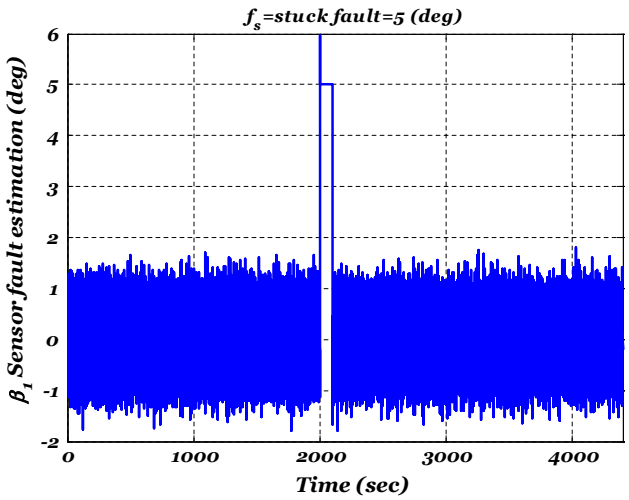

Fig. 10 Blade-1 stuck sensor fault estimation using PPIO

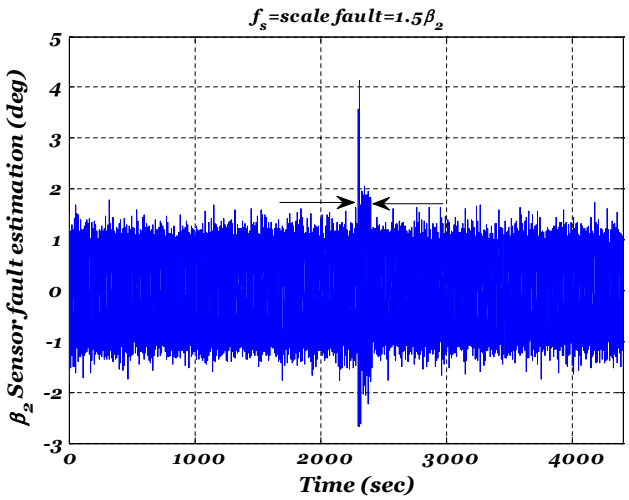

Fig. 11 Blade-2 scale sensor fault estimation using PPIO

to FTC (see Fig. 1). Figure 8 shows the sensor fault estimation accuracy.

The proposal has been tested using the realistic faults and wind data of the wind turbine FTC benchmark model [7]. The model represents a three-bladed variable-pitch variable-speed horizontal axis 4.8 MW wind turbine with a realistic wind model has been included that comprises stochastic wind behavior, wind shear effects, and tower shadow effects. In this benchmark model, it is required to tolerate the effects of sensor, actuator, and process faults in different parts of this benchmark model. For instance, it is important that the proposed FTC scheme be able to tolerate the parameter change and sensor faults of the pitch actuator system simultaneously since these faults will influence the pitch positions as demonstrated above. Figure 9 illustrate the effects of model parameter fault as well as the fault tolerance capability of the ISMC. In Figs. 10 and 11, fault estimation capability of the PPIO has been exploited to estimate blade-1 stuck sensor fault and blade-2 scale sensor fault separately. Additionally, the benefits of using the integrated ISMC and PPIO scheme to tolerate simultaneous actuator and sensor faults have been demonstrated in Fig. 12.

5 Conclusions

This paper proposes a robust sliding mode controller for pitch actuator system of wind turbine contaminated by actuator and sensor faults. The results have shown that the sliding mode controller is capable of compensating the effects of actuator faults. However, sensor fault has a direct effect on SMC performance since this fault affects the sliding variable and thereby the SMC signal steers the system to follow incorrect measurements. Subsequently, this paper proved that com-

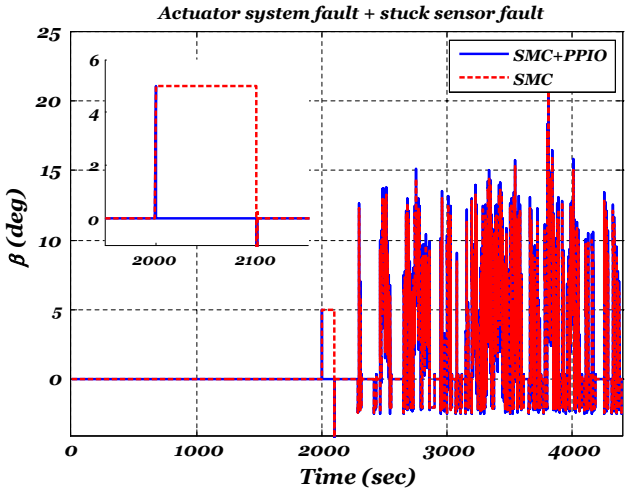

Fig. 12 The performance of integrated SMC+PPIO against simultaneous actuator system fault ($\zeta = 0.25\,\omega_n = 5.73\,\text{rad/s}$) and blade-1 stuck sensor fault

bining the SMC with PPIO solves the robustness problem of simultaneous actuator and sensor fault.

References

1. Luo, N.; Vidal, Y.; Acho, L.: Wind Turbine Control and Monitoring. Springer, Berlin (2014)
2. Bianchi, D.F.; de Battista, H.; Mantz, J.R.: Wind Turbine Control Systems: Principles, Modelling and Gain Scheduling Design. Springer, Berlin (2007)
3. Carriveau, R.: Fundamental and Advanced Topics in Wind Power. InTech, Rijeka (2011)
4. Badihi, H.; Zhang, Y.; Hong, H.: Fuzzy gain-scheduled active fault-tolerant control of a wind turbine. J. Frankl. Inst. **351**, 3677–3706 (2014)
5. Stewart, G.; Lackner, M.: Offshore wind turbine load reduction employing optimal passive tuned mass damping systems. IEEE Trans. Control Syst. Technol. **21**, 1090–1104 (2013)
6. Simani, S.; Castaldi, P.: Data-driven and adaptive control applications to a wind turbine benchmark model. Control Eng. Pract. **21**, 1678–1693 (2013)
7. Odgaard, P.F.; Stoustrup, J.; Kinnaert, M.: Fault-tolerant control of wind turbines: a benchmark model. IEEE Trans. Control Syst. Technol. **21**, 1168–1182 (2013)
8. Sami, M.; Patton, R.J.: Fault tolerant adaptive sliding mode controller for wind turbine power maximisation. Presented at the 7th IFAC Symposium on Robust Control Design, Aalborg Congress & Culture Centre, Denmark (2012)
9. Schulte, H.; Gauterin, E.: Fault-tolerant control of wind turbines with hydrostatic transmission using Takagi–Sugeno and sliding mode techniques. Annu. Rev. Control **40**, 82–92 (2015)
10. Simani, S.: Overview of modelling and advanced control strategies for wind turbine systems. Energies **8**, 12374 (2015)
11. Shi, F.; Patton, R.: An active fault tolerant control approach to an offshore wind turbine model. Renew. Energy **75**, 788–798 (2015)
12. Vidal, Y.; Tutivén, C.; Rodellar, J.; Acho, L.: Fault diagnosis and fault-tolerant control of wind turbines via a discrete time controller with a disturbance compensator. Energies **8**, 4300 (2015)
13. Sloth, C.; Esbensen, T.; Stoustrup, J.: Robust and fault-tolerant linear parameter-varying control of wind turbines. Mechatronics **21**, 645–659 (2011)
14. Sami, M.; Patton, R.J.: A fault tolerant control approach to sustainable offshore wind turbines. In: Luo, N., Vidal, Y., Acho, L. (eds.) Wind Turbine Control and Monitoring. Springer, Berlin (2014)
15. Shaker, M.S.; Patton, R.J.: Active sensor fault tolerant output feedback tracking control for wind turbine systems via T–S model. Eng. Appl. Artif. Intell. **34**, 1–12 (2014)
16. Benbouzid, M.; Beltran, B.; Amirat, Y.; Yao, G.; Han, J.; Mangel, H.: Second-order sliding mode control for DFIG-based wind turbines fault ride-through capability enhancement. ISA Trans. **53**, 827–833 (2014)
17. Sami, M.; Patton, R.J.: Wind turbine sensor fault tolerant control via a multiple-model approach. Presented at The 2012 UKACC International Conference on Control, Cardiff (2012)
18. Sami, M.; Patton, R. J.: An FTC approach to wind turbine power maximisation via T–S fuzzy modelling and control. In: 8th IFAC Symposium on Fault Detection, Supervision and Safety of Technical Processes, Mexico City, Mexico, pp. 349–354 (2012)
19. Odgaard, P.F.; Stoustrup, J.; Kinnaert, M.: Fault tolerant control of wind turbines: a benchmark model. Presented at the 7th IFAC Symposium on Fault Detection, Supervision and Safety of Technical Processes Safeprocess 2009, Barcelona (2009)
20. Edwards, C.; Spurgeon, S.: Sliding Mode Control: Theory and Applications. Taylor & Francis, London (1998)
21. Shaker, M.S.: Integral sliding mode approach to robust control systems against friction force. Arab. J. Sci. Eng. **41**, 3695–3702 (2016)
22. Shtessel, Y.; Christopher, E.; Leonid, F.; Arie, L.: Sliding Mode Control and Observation. Springer, Berlin (2014)
23. Shaker, M.S.: A robust adaptive observer-based time varying fault estimation. Amirkabir Int. J. Model. Identif. Simul. Control **47**, 11–19 (2015)
24. Hace, A.; Franc, M.: FPGA implementation of sliding-mode-control algorithm for scaled bilateral teleoperation. IEEE Trans. Ind. Inform. **9**, 1291–1300 (2013)
25. Sencer, B.; Mori, T.; Shamoto, E.: Design and application of a sliding mode controller for accurate motion synchronization of dual servo systems. Control Eng. Pract. **21**, 1519–1530 (2013)
26. Nise, N.S.: Control Systems Engineering, 6th edn. Wiley, New York (2011)